Atmospheric Chemistry of HFC-227ca: Spectrokinetic Investigation of the $CF_3CF_2CF_2O_2$ Radical, Its Reactions with NO and NO_2, and the Atmospheric Fate of the $CF_3CF_2CF_2O$ Radical

Anders M. B. Giessing,[†] Anders Feilberg,[†] Trine E. Møgelberg, Jens Sehested,* and Merete Bilde

Section for Chemical Reactivity, Environmental Science and Technology Department, Risø National Laboratory, DK-4000 Roskilde, Denmark

Timothy J. Wallington*

Ford Motor Company, Ford Research Laboratory, SRL-E3083, Dearborn, P.O. Box 2053, Michigan 48121-2053

Ole J. Nielsen*

Ford Motor Company, Ford Forschungszentrum Aachen, Dennewartstrasse 25, D-52068 Aachen, Germany

Received: September 20, 1995; In Final Form: January 22, 1996[⊗]

A pulse radiolysis technique was used to study the UV absorption spectrum of $CF_3CF_2CF_2O_2$ radicals, at 230 nm $\sigma = (3.2 \pm 0.4) \times 10^{-18}$ cm^2 molecule^{-1}. Rate constants for reactions of $CF_3CF_2CF_2O_2$ radicals with NO and NO_2 were $k_3 > 7 \times 10^{-12}$ cm^3 molecule^{-1} s^{-1} and $k_4 = (7.6 \pm 2.4) \times 10^{-12}$ cm^3 molecule^{-1} s^{-1}, respectively. The rate constant for reaction of F atoms with $CF_3CF_2CF_2H$ was determined by using an absolute rate technique to be $(3.6 \pm 1.3) \times 10^{-13}$ cm^3 molecule^{-1} s^{-1}. The atmospheric fate of $CF_3CF_2CF_2O$ radicals is decomposition via C−C bond scission to give CF_3CF_2 radicals and CF_2O. In one bar of SF_6 at 296 K, $CF_3CF_2CF_2O$ radicals decompose with a rate $> 1.5 \times 10^5$ s^{-1}. In their turn CF_3CF_2 radicals are converted into CF_3CF_2O radicals which also decompose via C−C bond scission. As part of this work a relative rate method was used to measure $k(Cl + CF_3CF_2CF_2H) = (3.4 \pm 0.7) \times 10^{-16}$ and $k(F + CF_3CF_2CF_2H) = (3.2 \pm 0.8) \times 10^{-13}$ cm^3 molecule^{-1} s^{-1}. The results are discussed with respect to the atmospheric chemistry of HFC-227ca.

Introduction

Recognition of the adverse impact of chlorofluorocarbons (CFCs) on stratospheric ozone has led to an international effort to replace CFCs with environmentally acceptable alternatives.[1] Hydrofluorocarbons (HFCs) are one class of CFC replacements used in refrigeration, air conditioning, foam blowing, and cleaning applications. HFC-227ca ($CF_3CF_2CF_2H$) is a potential CFC replacement and has a chemical structure which is similar to that of HFC-125 (CF_3CF_2H). HFC-125 is currently used in blends with HFC-134a (CF_3CH_2F) and HFC-32 (CF_2H_2) as a replacement for HCFC-22 ($CHClF_2$). Global production of up to 10 ktonnes per year of HFC-125 is expected[2] while current production of HFC-134a is approximately 150 ktonnes. There are no available estimates for the future production of HFC-227ca.

The atmospheric chemistry of HFC-227ca is of interest for two reasons. First, information concerning HFC-227ca is needed to determine its environmental impact. Second, in light of its structural similarity to HFC-125, information concerning HFC-227ca sheds light on the atmospheric chemistry of HFC-125 and indeed other HFCs. The main atmospheric loss mechanism for $CF_3CF_2CF_2H$ is expected to be reaction with OH radicals in the troposphere to produce a fluorinated alkyl radical which will react rapidly with O_2 to give $CF_3CF_2CF_2O_2$.

$$CF_3CF_2CF_2H + OH \rightarrow CF_3CF_2CF_2 + H_2O \quad (1)$$

$$CF_3CF_2CF_2 + O_2 + M \rightarrow CF_3CF_2CF_2O_2 + M \quad (2)$$

The rate constant for reaction 1 is unknown; however, the atmospheric lifetime of HFC-227ca can be estimated as 26 years from the lifetime of CF_3CF_2H as discussed in a later section.

By analogy to other peroxy radicals,[3] $CF_3CF_2CF_2O_2$ radicals are expected to react with NO, NO_2, HO_2, or other peroxy radicals in the atmosphere.

$$CF_3CF_2CF_2O_2 + NO \rightarrow CF_3CF_2CF_2O + NO_2 \quad (3a)$$

$$CF_3CF_2CF_2O_2 + NO + M \rightarrow CF_3CF_2CF_2ONO_2 + M \quad (3b)$$

$$CF_3CF_2CF_2O_2 + NO_2 + M \rightarrow CF_3CF_2CF_2O_2NO_2 + M \quad (4)$$

$$CF_3CF_2CF_2O_2 + HO_2 \rightarrow \text{products} \quad (5)$$

$$CF_3CF_2CF_2O_2 + R'O_2 \rightarrow \text{products} \quad (6)$$

A pulse radiolysis technique combined with UV−visible absorption spectroscopy was used to determine the UV absorption spectrum of $CF_3CF_2CF_2O_2$ and to study the kinetics of

* Authors to whom correspondence may be addressed.
[†] Present address: Roskilde University, Institute of Life Sciences and Chemistry, P. O. Box 260, DK-4000 Roskilde, Denmark.
[⊗] Abstract published in *Advance ACS Abstracts,* March 15, 1996.

0022-3654/96/20100-6572$12.00/0

reactions 3, 4, and 6. In the case of reaction 6 we studied the self reaction of the peroxy radical ($R' = CF_3CF_2CF_2$). The fate of the $CF_3CF_2CF_2O$ radical produced in reaction 3 was determined by using a FTIR spectrometer coupled to a smog chamber. The results are reported herein.

Experimental Section

The two experimental systems used in the present work are described in detail elsewhere.[4,5] All experiments were performed at 296 ± 2 K.

Pulse Radiolysis System. Radicals were generated by irradiation of $SF_6/CF_3CF_2CF_2H/O_2$ gas mixtures in a 1-L stainless steel reaction cell with a 30-ns pulse of 2 MeV electrons from a Febetron 705B field emission accelerator. SF_6 was always in great excess.

$$SF_6 + 2\ \text{MeV}\ e^- \rightarrow \text{products} \quad (7)$$

$$CF_3CF_2CF_2H + F \rightarrow CF_3CF_2CF_2 + HF \quad (8)$$

$$CF_3CF_2CF_2 + O_2 + M \rightarrow CF_3CF_2CF_2O_2 + M \quad (2)$$

Transient absorptions were followed by multipassing the output of a pulsed 150-W xenon arc lamp through the reaction cell using internal White cell optics. Total path lengths of 80 and 120 cm were used. After exiting the cell, the light was guided through a 1-m McPherson grating UV−vis monochromator and detected with a Hamamatsu photomultiplier. The spectral resolution was 0.8 nm. For the measurement of the UV absorption spectrum of the peroxy radical $CF_3CF_2CF_2O_2$ a Princeton Applied Research OMA-II diode array spectrophotometer was used in place of the photomultiplier. The system consisted of the diode array, an image amplifier (type 1420−1024HQ), a controller (type 1421), and a conventional PC computer for handling and storage of the data. Wavelength calibration was achieved by using a Hg pen ray lamp.

Reagent concentrations used were: SF_6, 895−950 mbar; O_2, 0−5 mbar; $CF_3CF_2CF_2H$, 0−100 mbar; NO, 0.20−0.71 mbar; and NO_2, 0.17−1.00 mbar. All experiments were performed at 296 K. Ultrahigh purity O_2 was supplied by L'Air Liquide. SF_6 (99.9%) was supplied by Gerling and Holz. $CF_3CF_2CF_2H$ (>97%) was obtained from PCR Inc. NO (99.8%) was obtained from Messer Grieshem. NO_2 (>98%) was obtained from Linde Technische Gase. All reagents were used as received.

Prior to the present series of experiments the F atom yield was determined by monitoring the transient absorbance at 260 nm due to methylperoxy radicals produced by pulse radiolysis of $SF_6/CH_4/O_2$ mixtures.[6] Using a value of 3.18×10^{-18} cm^2 molecule^{-1} for $\sigma(CH_3O_2)$ at 260 nm[7] the F atom yield was determined to be $(3.18 \pm 0.31) \times 10^{15}$ cm^{-3} at full radiolysis dose and 1000 mbar of SF_6. The quoted error on the F atom yield includes both statistical (2 standard deviations) and potential systematic errors associated with a 10% uncertainty in $\sigma(CH_3O_2)$. Errors are propagated by using conventional error analysis methods and are ±2 standard deviations if not otherwise stated.

Five sets of experiments were performed. First, the rate constant for reaction 8 was determined by observing the dependence of the absorbance maximum on the $[CF_3CF_2CF_2H]/[CF_3CCl_2H]$ concentration ratio following the pulse radiolysis of $SF_6/CF_3CF_2CF_2H/CF_3CCl_2H$ mixtures. Second, the diode array was used to measure the UV absorption spectrum of the $CF_3CF_2CF_2O_2$ radical following pulsed radiolysis of $SF_6/CF_3CF_2CF_2H/O_2$ mixtures. Third, the decay of $CF_3CF_2CF_2O_2$ was monitored to derive a value for the rate constant of its self-reaction. Fourth, the kinetics of the reaction of the peroxy radical with NO were determined by monitoring the kinetics of NO_2 formation following pulsed radiolysis of $SF_6/CF_3CF_2CF_2H/O_2/NO$ mixtures. Fifth, similar experiments were performed by using $SF_6/CF_3CF_2CF_2H/O_2/NO_2$ mixtures with the decay of NO_2 monitored to determine the kinetics of the reaction of $CF_3CF_2CF_2O_2$ radicals with NO_2.

FTIR Smog Chamber System. The FTIR (Fourier transform infrared) system was interfaced to a 140-L Pyrex reactor. Radicals were generated by the UV irradiation of mixtures of 13−30 mTorr of $CF_3CF_2CF_2H$, 21−26 mTorr of NO, and 700−715 mTorr of Cl_2 in either 5 or 10 Torr total pressure of O_2 diluent (760 Torr = 1013 mbar). UV light was provided by 22 blacklamps, which emit light between 300 and 400 nm. This light was used to produce Cl atoms from Cl_2. Cl atoms were used to initiate the reactions. The loss of reactants and the formation of products were monitored by FTIR spectroscopy, using an analyzing path length of 26 m and a resolution of 0.25 cm^{-1}. Infrared spectra were derived from 32 co-added spectra. $CF_3CF_2CF_2H$ and COF_2 were monitored by using their characteristic features over the wavenumber range 700−2000 cm^{-1}. Reference spectra were acquired by expanding known volumes of reference materials into the reactor.

Results

Kinetics of the Reaction F + $CF_3CF_2CF_2H$. The kinetics of the reaction of F atoms with $CF_3CF_2CF_2H$ were studied relative to the reaction of F atoms with CF_3CCl_2H by observing the maximum absorbance following pulse radiolysis of mixtures of 0−100 mbar of $CF_3CF_2CF_2H$ and 1−10 mbar of CF_3CCl_2H with SF_6 added to a total pressure of 1000 mbar. A relative radiolysis dose of 0.32 was used. Under these circumstances reactions 8 and 9 compete for F atoms:

$$F + CF_3CF_2CF_2H \rightarrow CF_3CF_2CF_2 + HF \quad (8)$$

$$F + CF_3CCl_2H \rightarrow CF_3CCl_2 + HF \quad (9)$$

The alkyl radical produced in reaction 9 (CF_3CCl_2) absorbs strongly at 230 nm,[8] whereas the radical produced in reaction 8 ($CF_3CF_2CF_2$) absorbs weakly. The competition between reactions 8 and 9 was studied by observing the dependence of the maximum absorbance at 230 nm on the $[CF_3CF_2CF_2H]/[CF_3CCl_2H]$ concentration ratio following pulsed radiolysis of $CF_3CF_2CF_2H/CF_3CCl_2H/SF_6$ mixtures. In Figure 1 the maximum absorbance is plotted as a function of the $[CF_3CF_2CF_2H]/[CF_3CCl_2H]$ concentration ratio. In the absence of $CF_3CF_2CF_2H$ all F atoms are converted into CF_3CCl_2 radicals via reaction 9 and the transient absorption at 230 nm is substantial. When $CF_3CF_2CF_2H$ is added, F atoms are scavenged by reaction 8 and the transient absorption attributed to CF_3CCl_2 radicals decreases. The maximum absorbance decreases until the $[CF_3CF_2CF_2H]/[CF_3CCl_2H]$ ratio is approximately 25. Increasing the ratio further has little impact on the maximum absorbance. To obtain the rate constant ratio k_8/k_9 the following expression was fitted to the data in Figure 1:

$$A_{max} = \{A_{CF_3CCl_2} + A_{CF_3CF_2CF_2}(k_8/k_9)[CF_3CF_2CF_2H]/[CF_3CCl_2H]\}/\{1 + (k_8/k_9)[CF_3CF_2CF_2H]/[CF_3CCl_2H]\}$$

A_{max} is the measured maximum absorbance, $A_{CF_3CCl_2}$ is the expected absorbance if only CF_3CCl_2 radicals were produced,

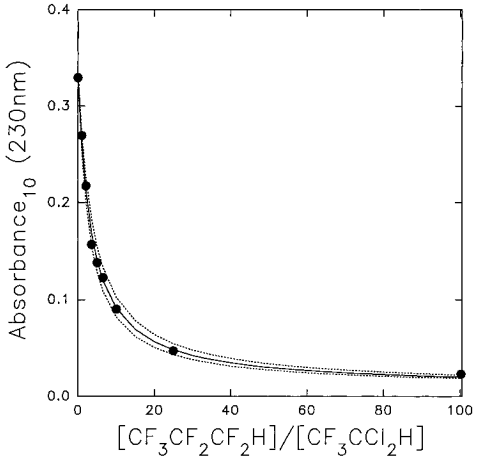

Figure 1. Plot of maximum transient absorbance at 230 nm as a function of the concentration ratio $[CF_3CF_2CF_2H]/[CF_3CCl_2H]$, following the radiolysis of mixtures of 0−100 mbar of $CF_3CF_2CF_2H$, 10 mbar of CF_3CCl_2H, and 990 mbar of SF_6. The UV path length was 80 cm and radiolysis dose was 32% of maximum. The smooth line and the dotted lines are fit to the data. See text for details.

and $A_{CF_3CF_2CF_2}$ is the expected absorbance if only $CF_3CF_2CF_2$ radicals were produced. The rate constant ratio k_8/k_9 was derived by performing a three parameter fit to the data in Figure 1 in which the parameters $A_{CF_3CCl_2}$, $A_{CF_3CF_2CF_2}$, and k_8/k_9 were varied simultaneously. The fit is shown as the solid line in Figure 1 and was achieved with $k_8/k_9 = 0.30 \pm 0.05$. The dotted lines in Figure 1 show the effects of varying k_8/k_9 by $\pm$ 0.05. Using $k_9 = (1.2 \pm 0.4) \times 10^{-12}$ [9] gives $k_8 = (3.6 \pm 1.3) \times 10^{-13}$, in agreement with a value of $k_8 = (3.2 \pm 0.8) \times 10^{-13}$ cm^3 $molecule^{-1}$ s^{-1} measured by using a relative rate technique described in a subsequent section of the present paper.

Absorption Spectrum of $CF_3CF_2CF_2O_2$. Following the pulse radiolysis (full dose) of mixtures of 5 mbar of O_2, 50 mbar of $CF_3CF_2CF_2H$, and 945 mbar of SF_6 a rapid increase in the absorption at 230 nm was observed followed by a slower decay (see Figure 2). It seems reasonable to ascribe the UV absorption resulting from radiolysis of $SF_6/CF_3CF_2CF_2H/O_2$ mixtures to the formation of $CF_3CF_2CF_2O_2$ radicals. Before measuring the absorption cross sections of the $CF_3CF_2CF_2O_2$ radical we need to consider possible interfering secondary reactions.

After the electron pulse reactions, (8) and (10) compete for the available F atoms.

$$F + CF_3CF_2CF_2H \rightarrow CF_3CF_2CF_2 + HF \quad (8)$$

$$F + O_2 + M \rightarrow FO_2 + M \quad (10)$$

By use of $k_8 = (3.6 \pm 1.3) \times 10^{-13}$ cm^3 $molecule^{-1}$ s^{-1} (see previous section) and $k_{10} = (1.9 \pm 0.3) \times 10^{-13}$ cm^3 $molecule^{-1}$ s^{-1},[6] it can be calculated that under our experimental conditions 95% of F atoms are converted into $CF_3CF_2CF_2O_2$ and 5% into FO_2 radicals.

We also need to consider possible interfering secondary reactions such as

$$F + CF_3CF_2CF_2 \rightarrow \text{products} \quad (11)$$

$$F + CF_3CF_2CF_2O_2 \rightarrow \text{products} \quad (12)$$

$$CF_3CF_2CF_2O_2 + CF_3CF_2CF_2 \rightarrow 2CF_3CF_2CF_2O \quad (13)$$

To check for these reactions, a set of experiments was performed using mixtures of 5 mbar of O_2, 50 mbar of $CF_3CF_2CF_2H$, and 945 mbar of SF_6 with the radiolysis dose varied over an order of magnitude. In Figure 3 the maximum transient absorbance observed at 230 nm using a path length of 120 cm is plotted as a function of radiolysis dose. As seen from Figure 3, the maximum absorbance was linear up to 42% of maximum radiolysis dose. At higher doses the observed absorbance was smaller than expected from a linear extrapolation of the low dose experiments. We ascribe the curvature to incomplete conversion of F atoms into $CF_3CF_2CF_2O_2$ and FO_2 radicals caused by secondary radical−radical reactions, such as reactions 11−13. The solid line shown in Figure 3 is a linear least squares fit of the low dose data. The slope is (0.515 ± 0.031). Combining this result with three additional pieces of information, (i) the F atom yield of $(3.18 \pm 0.31) \times 10^{15}$ cm^{-3} (full radiolysis dose and 1000 mbar of SF_6), (ii) the conversion of F atoms into 95% $CF_3CF_2CF_2O_2$ and 5% FO_2 radicals, and (iii) the absorption cross section for FO_2 at 230 nm ($\sigma_{230} = 5.08 \times 10^{-18}$ cm^2 $molecule^{-1}$),[6] we derive $\sigma(CF_3CF_2CF_2O_2)$ at 230 nm

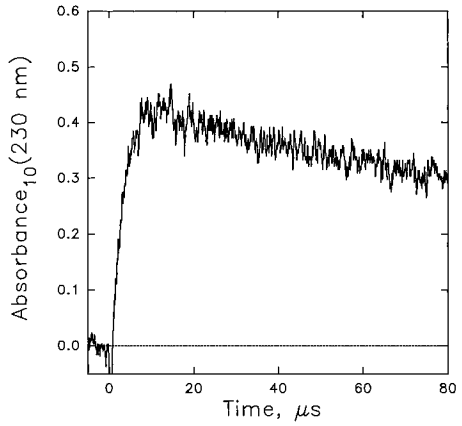

Figure 2. Transient absorption at 230 nm following the pulsed radiolysis (full dose) of a mixture of 5 mbar of O_2, 50 mbar of $CF_3CF_2CF_2H$, and 945 mbar of SF_6. An UV path length of 120 cm was used.

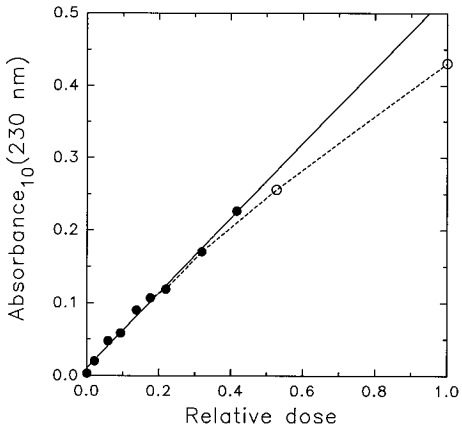

Figure 3. Maximum transient absorbance as a function of radiolysis dose at 230 nm following the pulse radiolysis of mixtures of 5 mbar of O_2, 50 mbar of $CF_3CF_2CF_2H$, and 945 mbar of SF_6. The solid line is a linear fit to the low dose data, the dotted curve is a second order regression of all the data to aid in visual inspection of the data trend.

TABLE 1: Measured UV Absorption Cross Sections

wavelength, nm	$\sigma(CF_3CF_2CF_2O_2)$ 10^{-20} cm^2 $molecule^{-1}$	wavelength, nm	$\sigma(CF_3CF_2CF_2O_2)$ 10^{-20} cm^2 $molecule^{-1}$
230	320	250	82
235	252	255	65
240	152	260	23
245	125	270	16

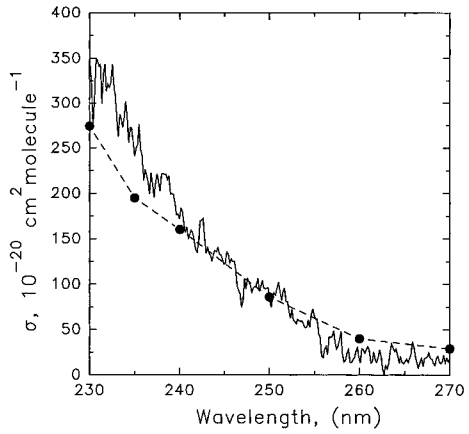

Figure 4. Absorption spectrum of $CF_3CF_2CF_2O_2$ measured in this work (solid line) compared to that of $CF_3CF_2O_2$ (circles and dashed line).[23]

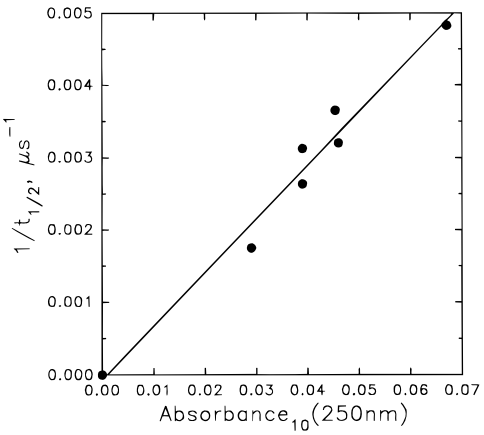

Figure 5. Plot of $1/t_{1/2}$ for the self-reaction of $CF_3CF_2CF_2O_2$ as a function of maximum absorbance at 250 nm.

$= (3.2 \pm 0.4) \times 10^{-18}$ cm^2 molecule^{-1}. A full spectrum of $CF_3CF_2CF_2O_2$ absorption cross sections between 230 and 270 nm is shown in Figure 4. The spectrum was obtained by recording the absorbance following pulse radiolysis (full dose) of mixtures of 50 mbar of $CF_3CF_2CF_2H$, 5 mbar of O_2, and 945 mbar of SF_6 using a diode array camera under the following conditions: spectral resolution, 2 nm; gate, 20 μs; delay, 5 μs. The observed absorbance values were corrected for FO_2 absorbance by using the absorption cross sections measured by Ellermann et al.[6] and then scaled to σ_{230nm} ($CF_3CF_2CF_2O_2$) $= 3.2 \times 10^{-18}$ cm^2 molecule^{-1}.

The UV spectrum of $CF_3CF_2CF_2O_2$ measured in the present work is compared to that for $CF_3CF_2O_2$ in Figure 4. As expected for such similar peroxy radicals their spectra are, within the experimental uncertainties, indistinguishable.

Kinetics of the Self-Reaction of $CF_3CF_2CF_2O_2$. Pulsed radiolysis of $CF_3CF_2CF_2H/O_2/SF_6$ gas mixtures gave rise to an increase in the transient absorbance at 250 nm caused by formation of peroxy radicals. The maximum absorbance was reached within a few microseconds after the electron pulse, subsequently a slower decay in the transient absorbance was observed. It seems reasonable to ascribe the decay in absorbance to the self reaction of the peroxy radicals.

$$CF_3CF_2CF_2O_2 + CF_3CF_2CF_2O_2 \rightarrow \text{products} \quad (14)$$

The kinetic expression for reaction 14 is $d[RO_2]/dt = -2k_{14obs}[RO_2]^2$, where k_{14obs} is the observed second order rate constant for reaction 14. The half-life of reaction 14 is defined as $t_{1/2} = 1/(2k_{14obs}[RO_2])$. Using Lambert−Beers law, we get $1/t_{1/2} = 2.303A_{max}2k_{14obs}/80\sigma_{RO_2})$. The half-life of reaction 14 can be obtained by fitting the following second order expression to the observed decay in the transient absorbance: $A(t) = (A_0 - A_{inf})/(1 + 2k_{14obs}(A_0 - A_{inf})t) + A_{inf}$, where $A(t)$ is the measured absorbance at time t, A_0 is the absorbance at time zero and A_{inf} is the absorbance at infinite time. Since σ_{RO_2} has been determined (see preceding section), k_{14obs} can be derived by plotting the reciprocal half-life versus A_{max}. This plot is shown in Figure 5 with a linear least squares regression of the data points. The different data points were obtained by using different radiolysis doses. Figure 5 shows a plot of $1/t_{1/2}$ versus the maximum absorbance attributable to $CF_3CF_2CF_2O_2$ radicals. The slope of the plot in Figure 5 equals $2k_{14obs}2.303/(80\sigma_{RO_2}(250))$ and gives $k_{14obs} = (1.0 \pm 0.2) \times 10^{-12}$ cm^{-3} molecule^{-1} s^{-1}. The self reaction of $CF_3CF_2CF_2O_2$ radicals gives $CF_3CF_2CF_2O$ radicals, which, as we will show in a later section, decompose rapidly to give CF_3CF_2 radicals and COF_2. CF_3CF_2 radicals will add O_2 to give $CF_3CF_2O_2$ radicals. The formation of $CF_3CF_2O_2$ radicals poses two problems in terms of the interpretation of k_{14obs}. First, since they absorb at the monitoring wavelength of 250 nm (see Figure 4), the formation of $CF_3CF_2O_2$ radicals masks the loss of $CF_3CF_2CF_2O_2$ radicals. Second, $C_2F_5O_2$ radicals will react with $CF_3CF_2CF_2O_2$ radicals hence complicating the kinetic analysis. At the present time we are unable to correct k_{14obs} for such complications and so we are unable to derive a value for the true bimolecular rate constant k_{14}. The value of k_{14obs} reported here is the observed rate constant for decay of absorption at 250 nm.

Kinetics of the $CF_3CF_2CF_2O_2$ + NO Reaction. The kinetics of reaction 3 were studied by measuring the transient absorbance at 400 nm following pulse radiolysis of mixtures of 100 mbar of $CF_3CF_2CF_2H$, 5 mbar of O_2, 0.20−0.71 mbar of NO, and SF_6 added to a total pressure of 1000 mbar.

$$CF_3CF_2CF_2O_2 + NO \rightarrow CF_3CF_2CF_2O + NO_2 \quad (3a)$$

$$CF_3CF_2CF_2O_2 + NO + M \rightarrow CF_3CF_2CF_2ONO_2 + M \quad (3b)$$

An increase in the transient absorbance following pulse radiolysis was observed, and, since NO_2 is known to absorb significantly at 400 nm, we ascribe the observed increase in absorbance to formation of NO_2 in reaction 3a. This method of measuring the kinetics of the reaction of peroxy radicals with NO has been used extensively in our laboratory and is described in detail elsewhere.[10−13]

The transient absorbancies were fitted by using the first order expression $A(t) = (A_{inf} - A_0) \exp(-k^{1st}t) + A_{inf}$ with the fit starting 3 μs after the electron pulse to allow time for formation of the peroxy radicals. Figure 6A shows a typical transient absorption, the smooth line is the first order fit with a pseudo-first-order rate constant $k^{1st} = 0.95 \times 10^5$ s^{-1}. The bimolecular rate constant was derived by plotting the pseudo-first-order rate constants versus $[NO]_o$ as shown in Figure 7. Linear least squares analysis of the data in Figure 7 gives $k_3 = (8.1 \pm 1.1) \times 10^{-12}$ cm^3 molecule^{-1} s^{-1}; the y-axis intercept is $(0.9 \pm 1.3) \times 10^5$ s^{-1} and is not significant.

The yield of NO_2 in these experiments, expressed in terms of the initial F atom concentration, calculated by using σ_{NO2}(400 nm)$= 6 \times 10^{-19}$ cm^2 molecule^{-1},[14] was 182 ± 16%. Corrections were made for the consumption of F atoms by reaction with O_2 and NO, $k_{F+NO} = 5.1 \times 10^{-12}$ cm^3 molecule^{-1} s^{-1} (average from refs 15 and 16). The fact that the NO_2 yield is greater than 100% can be explained by the formation of NO_2 via reactions of NO with decomposition products of the alkoxy radical $CF_3CF_2CF_2O$ (see subsequent section). The decomposition of $CF_3CF_2CF_2O$ leads to CF_3CF_2 radicals, which can add

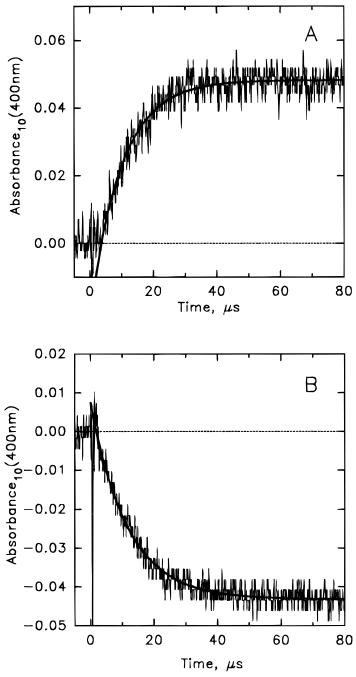

Figure 6. Transient absorbancies at 400 nm following pulsed radiolysis of mixtures of 100 mbar of $CF_3CF_2CF_2H$, 5 mbar of O_2, 940 mbar of SF_6, and either 0.5 mbar of NO and 32% radiolysis dose (A) or 0.2 mbar of NO_2 and 53% radiolysis dose (B). The UV path length was 120 cm.

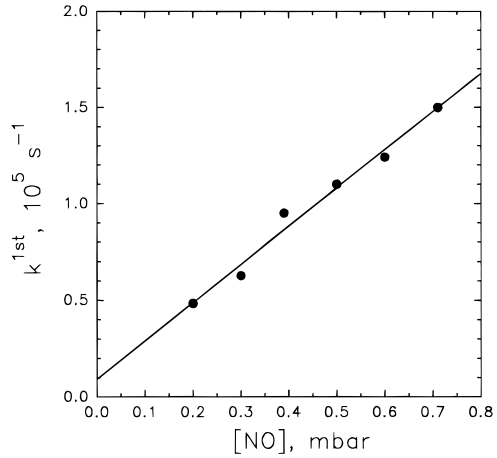

Figure 7. Plot of k^{1st} versus [NO].

O_2 to give another peroxy radical. $CF_3CF_2O_2$ will react with another NO in the system to give NO_2. The product, CF_3CF_2O, also falls apart to give CF_3 radicals and CF_2O. CF_3 radicals can add O_2 and the following reaction of CF_3O_2 can then produce another NO_2. In spite of this complicated mechanism, in all experiments the rise in the transient absorption at 400 nm followed first order kinetics. It follows that the rate of decomposition of $CF_3CF_2CF_2O$ radicals must be faster than the fastest pseudo-first-order rate measured, i.e., $>1.5 \times 10^5$ s^{-1}.

The formation of NO_2 from reactions which occur subsequent to reaction 3 introduces a delay in the overall appearance of NO_2. The value of $k_3 = (8.1 \pm 1.1) \times 10^{-12}$ determined in the present work should be regarded as a lower limit, hence, $k_3 > 7.0 \times 10^{-12}$ cm^3 $molecule^{-1}$ s^{-1}. This value is consistent with rate constants for other peroxy radicals derived from alkanes[7] and HFCs with respect to reaction with NO. For $CF_3CF_2O_2$, $k > (1.07 \pm 0.15) \times 10^{-11}$, for $CF_3CF_2CFHO_2$, $k > 8 \times 10^{-12}$,[17] for CF_3CFHO_2, $k = (1.31 \pm 0.41) \times 10^{-11}$,[18] and for $CF_3CH_2O_2$, $k = (1.2 \pm 0.3) \times 10^{-11}$ cm^3 $molecule^{-1}$ s^{-1}.[11]

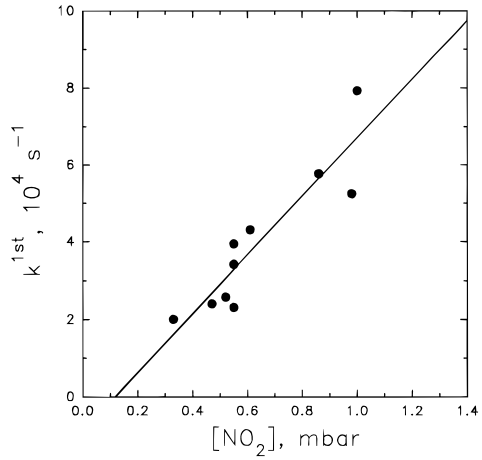

Figure 8. Plot of k^{1st} versus [NO_2].

Kinetics of the $CF_3CF_2CF_2O_2$ + NO_2 Reaction. The kinetics of reaction 4 were studied by measuring the transient absorbance at 400 nm following pulse radiolysis (53% of maximum dose) of mixtures of 100 mbar of $CF_3CF_2CF_2H$, 5 mbar of O_2, and 0.17−1.0 mbar of NO_2 with SF_6 added to a total pressure of 1000 mbar.

$$CF_3CF_2CF_2O_2 + NO_2 + M \rightarrow CF_3CF_2CF_2O_2NO_2 + M \quad (4)$$

In these experiments a decay in absorbance was observed following the radiolysis pulse. Since NO_2 absorbs at 400 nm, it seems reasonable to ascribe the decay to loss of NO_2 through reaction 4. This method of measuring the kinetics of the reaction of peroxy radicals with NO_2 has been used extensively in our laboratory and is described in detail elsewhere.[10,11,17,19]

Figure 6B shows an example of the decrease in the transient absorbance following pulse radiolysis (53% of maximum dose) of 100 mbar of $CF_3CF_2CF_2H$, 5 mbar of O_2, and 0.2 mbar of NO_2, with SF_6 added to a total pressure of 1000 mbar. The transient absorbancies were fitted by using the expression [Abs]-(t) = [Abs](0) $\exp(-k^{1st}t) + C$ where [Abs]$(t) + C$ and [Abs]-$(0) + C$ are the absorbance values at times t and 0, respectively, due to NO_2 and $k^{1st} = k_4[NO_2]$. The fit was started from 3 μs after the electron pulse to allow time for formation of the peroxy radicals. The resulting k^{1st} values are plotted versus $[NO_2]_o$ in Figure 8. The line in Figure 8 is a linear least squares regression of the data points, the slope gives $k_4 = (7.6 \pm 2.4) \times 10^{-12}$ cm^3 $molecule^{-1}$ s^{-1}. The y-axis intercept is not statistically significant.

Two reactions other than reaction 4 could be responsible for loss of NO_2:

$$F + NO_2 + M \rightarrow FNO_2/FONO + M \quad (15)$$

$$CF_3CF_2CF_2 + NO_2 \rightarrow \text{products} \quad (16)$$

In the presence of 100 mbar of $CF_3CF_2CF_2H$, F atoms have a lifetime of 1.3 μs. The absorption transients were fit from 3 μs after the radiolysis pulse reaction and hence reaction 15 will not be a complication. Reactions 16 competes with reaction 2 for the available $CF_3CF_2CF_2$ radicals. While the rate constant for reaction 2 has not been measured, it is very likely to be similar to that for the $CF_3 + O_2$ addition reaction, which has a high pressure limit of 4.0×10^{-12} cm^3 $molecule^{-1}$ s^{-1}.[20] Hence, the lifetime of $CF_3CF_2CF_2$ radicals in the presence of 5 mbar of O_2 is 2 μs and conversion of $CF_3CF_2CF_2$ into the peroxy radical will be substantially complete by the start of the data analysis at 3 μs after the radiolysis pulse. Complications caused

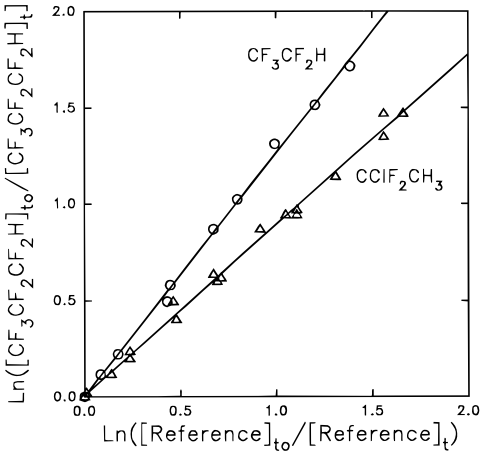

Figure 9. Loss of $CF_3CF_2CF_2H$ versus those of CF_3CF_2H and $CClF_2CH_3$ when mixtures containing these compounds were exposed to Cl atoms in 700 Torr of N_2 diluent.

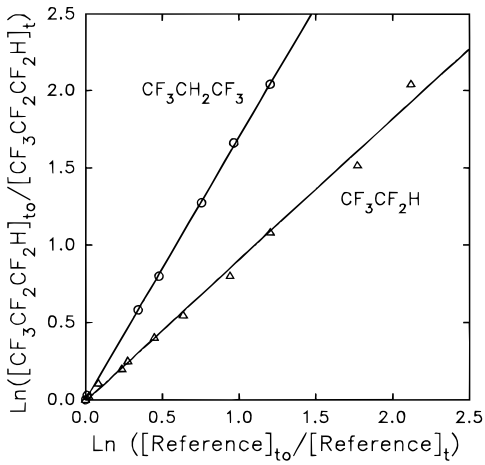

Figure 10. Loss of $CF_3CF_2CF_2H$ versus those of CF_3CF_2H and $CF_3CH_2CF_3$ when mixtures containing these compounds were exposed to F atoms in 700 Torr of N_2 diluent.

by reaction 16 should manifest themselves as curves in the plot of k_{1st} versus $[NO_2]$. Within the admittedly large data scatter in Figure 8 there is no such trend and we believe it reasonable to conclude that reaction 16 is not a significant complication.

The value of k_4 determined in this work is entirely consistent with the high pressure limiting rate constants for reactions between other halogenated peroxy radicals and NO_2 which lie in the range $(4.5-8.9) \times 10^{-12}$ cm^3 molecule^{-1} s^{-1}.[21]

Relative Rate Studies of the Reactions of Cl and F Atoms with $CF_3CF_2CF_2H$. Prior to investigating the atmospheric fate of $CF_3CF_2CF_2O$ radicals, a series of relative rate experiments were performed using the FTIR system to investigate the kinetics of reactions 18 and 8. The techniques used are described in detail elsewhere.[22]

Photolysis of molecular halogen was used as a source of halogen atoms.

$$Cl_2 \text{ (or } F_2) + h\nu \rightarrow 2Cl \text{ (or 2F)} \quad (17)$$

$$Cl + CF_3CF_2CF_2H \rightarrow CF_3CF_2CF_2 + HCl \quad (18)$$

$$F + CF_3CF_2CF_2H \rightarrow CF_3CF_2CF_2 + HF \quad (8)$$

The rate of reaction 18 was measured relative to (19) and (20). Reaction 8 was measured relative to (21) and (22).

$$Cl + CF_3CHF_2 \text{ (HFC-125)} \rightarrow \text{products} \quad (19)$$

$$Cl + CClF_2CH_3 \text{ (HCFC-142b)} \rightarrow \text{products} \quad (20)$$

$$F + CF_3CHF_2 \text{ (HFC-125)} \rightarrow CF_3CF_2 + HF \quad (21)$$

$$F + CF_3CH_2CF_3 \text{ (HFC-236fa)} \rightarrow CF_3CHCF_3 + HF \quad (22)$$

The observed losses of $CF_3CF_2CF_2H$ versus those of reference compounds in the presence of either Cl or F atoms are shown in Figures 9 and 10, respectively. All experiments were performed in 700 Torr of N_2 diluent. Linear least squares analysis gives $k_{18}/k_{19} = 1.26 \pm 0.06$, $k_{18}/k_{20} = 0.89 \pm 0.05$, $k_8/k_{21} = 0.91 \pm 0.05$, and k_8/k_{22}=1.70 $\pm$ 0.10. Using $k_{19} = 2.5 \times 10^{-16}$,[23] $k_{20} = 3.9 \times 10^{-16}$,[22] $k_{21} = 3.5 \times 10^{-13}$,[9] and $k_{22} = 1.8 \times 10^{-13}$ [12] gives $k_{18} = (3.15 \pm 0.15) \times 10^{-16}$, $k_{18} = (3.47 \pm 0.19) \times 10^{-16}$, $k_8 = (3.18 \pm 0.17) \times 10^{-13}$, and $k_8 = (3.06 \pm 0.64) \times 10^{-13}$ cm^3 molecule^{-1} s^{-1}, respectively. We estimate that potential systematic errors associated with uncertainties in the Cl and F reference rate constants could add additional 15% and 20% uncertainty ranges for k_{18} and k_8, respectively. Propagating these additional uncertainties gives values of $k_{18} = (3.2 \pm 0.5) \times 10^{-16}$, $k_{18} = (3.5 \pm 0.6) \times 10^{-16}$, $k_8 = (3.2 \pm 0.7) \times 10^{-13}$, and $k_8 = (3.1 \pm 0.6) \times 10^{-13}$ cm^3 molecule^{-1} s^{-1}. We choose to cite final values of k_{18} and k_8 which are averages of those determined by using the different reference compounds together with error limits which encompass the extremes of the individual determinations. Hence, $k_{18} = (3.4 \pm 0.7) \times 10^{-16}$ and $k_8 = (3.2 \pm 0.8) \times 10^{-13}$ cm^3 molecule^{-1} s^{-1}. Quoted errors reflect the accuracy of our measurements. The value of k_8 determined using the FTIR technique is in agreement with the determination of $k_8 = (3.6 \pm 1.3) \times 10^{-13}$ cm^3 molecule^{-1} s^{-1} from the pulse radiolysis technique in the present work. There are no literature data available for k_{18} or k_8 with which to compare our results.

Study of the Atmospheric Fate of $CF_3CF_2CF_2O$ Radicals. To determine the atmospheric fate of the alkoxy radical $CF_3CF_2CF_2O$ formed in reaction, 3 experiments were performed in which mixtures of 13−30 mTorr of $CF_3CF_2CF_2H$, 21−26 mTorr of NO, and 700−715 mTorr of Cl_2 in either 5 or 10 Torr total pressure of O_2 diluent were irradiated in the FTIR−smog chamber system. Loss of HFC-227ca and product formation were monitored by using FTIR spectroscopy. Only one carbon containing product was observed; COF_2. Figure 11 shows IR spectra acquired before (A) and after (B) a 103 min irradiation of a mixture of 29.3 mTorr of $CF_3CF_2CF_2H$, 21.0 mTorr of NO, and 697 mTorr of Cl_2 in 10 Torr of O_2. Panel C in Figure 11 shows the product spectrum derived by subtracting the IR features attributable to $CF_3CF_2CF_2H$ from panel B. Comparison of the product spectrum with a reference spectrum of COF_2 given in panel D shows that COF_2 is a major product. After subtracting COF_2 features there were no residual IR features which could be attributable to any other carbon containing products.

Figure 12 shows a plot of the formation of COF_2 versus the loss of $CF_3CF_2CF_2H$ observed in the present experiments. Individual variation of the $CF_3CF_2CF_2H$ partial pressure and the O_2 diluent pressure by factors of 2 had no discernible impact on the COF_2 yield. Linear least squares analysis of the data in Figure 11 gives a molar COF_2 yield of 272 $\pm$ 15%; i.e., COF_2 product accounts for 91 $\pm$ 5% of the loss of $CF_3CF_2CF_2H$. The shortfall of approximately 9% in the carbon balance may reflect the presence of some undetected product or systematic uncertainties in the determination of the COF_2 yield or both.

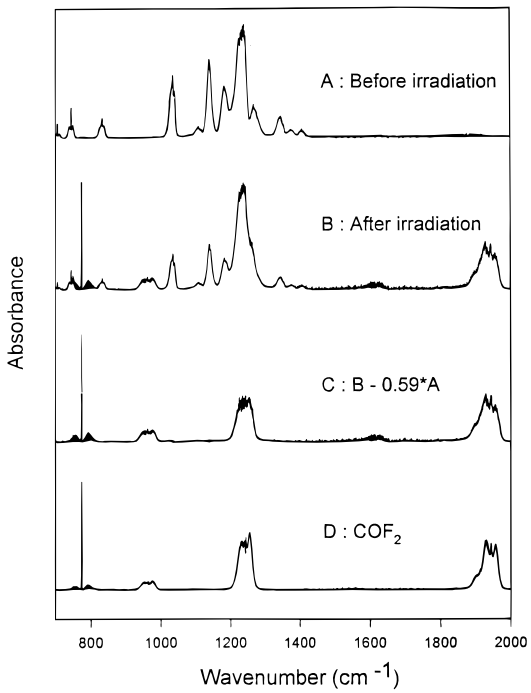

Figure 11. Infrared spectra acquired before (A) and after (B) irradiation of a mixture of $CF_3CF_2CF_2H/Cl_2/NO$ in O_2 diluent (see text for details). Panel C shows the result of subtracting features attributable to $CF_3CF_2CF_2H$ from panel B. Panel D is a reference spectrum of COF_2.

The observed COF_2 yield is consistent with the following reactions occurring in the chamber:

$$CF_3CF_2CF_2O_2 + NO \rightarrow CF_3CF_2CF_2O + NO_2 \quad (3a)$$

$$CF_3CF_2CF_2O + M \rightarrow CF_3CF_2 + COF_2 + M \quad (23)$$

$$CF_3CF_2 + O_2 + M \rightarrow CF_3CF_2O_2 + M \quad (24)$$

$$CF_3CF_2O_2 + NO \rightarrow CF_3CF_2O + NO_2 \quad (25a)$$

$$CF_3CF_2O + M \rightarrow CF_3 + COF_2 + M \quad (26)$$

$$CF_3 + O_2 + M \rightarrow CF_3O_2 + M \quad (27)$$

$$CF_3O_2 + NO \rightarrow CF_3O + NO_2 \quad (28a)$$

$$CF_3O + NO \rightarrow FNO + COF_2 \quad (29)$$

The observation of essentially complete conversion of $CF_3CF_2CF_2H$ into COF_2 allows several interesting conclusions. First, we can conclude that the atmospheric fate of the $CF_3CF_2CF_2O$ radical is C−C bond scission (reaction 23). This result is expected and is consistent with the determination from the pulse radiolysis experiments that reaction 23 proceeds with a rate greater than 1.5×10^5 s^{-1} at 296 K in 1 bar of SF_6. Second, we can confirm previous findings from this laboratory[23] and elsewhere[24,25] that C−C bond scission is the atmospheric fate of the alkoxy radical derived from HFC-125 (CF_3CF_2H). Third, we conclude that nitrate formation (e.g., reaction 3b) in the reaction of perfluoro alkyl peroxy radicals with NO is of minor importance. If we assume that CF_3O_2, $CF_3CF_2O_2$, and $CF_3CF_2CF_2O_2$ radicals all display the same tendency to form nitrates in their reaction with NO, then the 91 ± 5% carbon balance implies the nitrate yield in each of these reactions is <5%. This finding is consistent with the behavior of the analogous alkyl peroxy radicals which display little (e.g., 2% nitrate for n-$C_3H_7O_2$) tendency to form nitrates in their reactions with NO.[26]

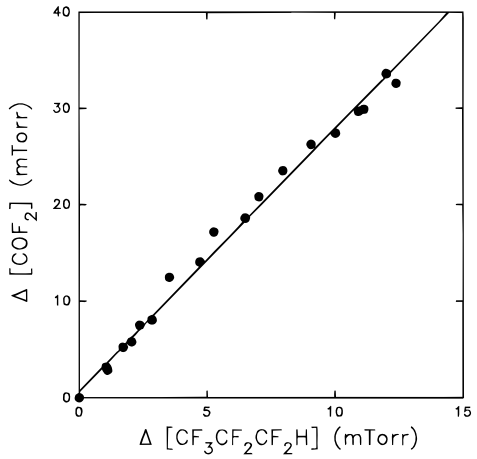

Figure 12. Yield of COF_2 versus the loss of $CF_3CF_2CF_2H$ following irradiation of $CF_3CF_2CF_2H/Cl_2/NO$ mixtures in O_2 diluent (see text for details).

Implications for Atmospheric Chemistry. Like all HFCs, the atmospheric lifetime of HFC-227ca will be determined by its rate of reaction with OH radicals. To the best of our knowledge there are no data available for the kinetics of the reaction of OH radicals with HFC-227ca. In the present work we show that HFC-227ca and HFC-125 have comparable reactivities toward Cl and F atoms. This finding is not unexpected when one considers the close similarity in the molecular structure of these two HFCs. It seems reasonable to expect that OH radicals will react with HFC-227ca at a rate which is comparable to their reaction with HFC-125. Percival et al.[27] have reported a correlation between the reactivity of HFCs towards OH radicals and the HFC ionization potential. HFC-227ca and HFC-125 have very similar ionization potentials (13.62 and 13.85 eV, respectively[27]), supporting the notion that HFC-227ca and HFC-125 will have similar reactivities toward OH radicals. Hence, the atmospheric lifetime of HFC-227ca will be similar to that of HFC-125; approximately 26 years.[28] Reaction of OH radicals with HFC-227ca in air gives $CF_3CF_2CF_2O_2$ radicals. In the present work it has been shown that in the presence of NO, $CF_3CF_2CF_2O_2$ radicals are converted into 2 molecules of COF_2 and a CF_3O radical. In the atmosphere CF_3O radicals react with hydrocarbons and NO to give CF_3OH and COF_2, respectively. The atmospheric fates of COF_2 and CF_3OH are dominated by incorporation into cloud−rain−sea water followed by hydrolysis to give HF and CO_2.[3]

The present work represents the first study of the atmospheric degradation of HFC-227ca. As expected, the behavior of HFC-227ca is very similar to that of HFC-125 (CF_3CF_2H). The reactivities of both HFCs toward F and Cl atoms are comparable. The spectra of the peroxy radicals generated from both HFCs and their reactivity of the peroxy radicals toward NO and NO_2 are indistinguishable. Once initiated by OH radical attack a sequence of rapid reactions occurs which results in the "unzipping" of the molecule in which successive COF_2 molecular fragments are shed and a CF_3 radical is formed. From the viewpoint of assessing the environmental acceptability of HFC-227ca as a CFC replacement, we must consider potential impact in three areas: stratospheric ozone depletion, toxic/noxious degradation product formation, and global warming. As with all HFCs, HFC-227ca has no impact on stratospheric ozone.[29] We show here that HFC-227ca is degraded into COF_2 and CF_3OH, neither of which can be considered toxic or noxious at the concentrations expected in the environment. The global warm-

ing potential of HFC-227ca is expected to be comparable to that of HFC-125, which (assuming a 100 year time horizon) is approximately 3200 times more effective at trapping infrared radiation than the same mass of CO_2.[30] To place this value in perspective it should be noted that CFC-11 and CFC-12 have global warming potentials which over a 100 year time horizon are factors of 4000 and 8500 larger than CO_2, respectively.[30]

References and Notes

(1) Alternative Fluorocarbon Environmental Acceptability Study, World Meteorological Organization Global Ozone Research and Monitoring Project, Report No. 20; *Scientific Assessment of Stratospheric Ozone*; 1989; Vol. I and II.

(2) McCulloch, A. *Environ. Monit. Assess.* **1994**, *31*, 167.

(3) Wallington, T. J.; Schneider, W. F.; Worsnop, D. R.; Nielsen, O. J.; Sehested J.; Debruyn, W. J.; Shorter, J. A. *Environ. Sci. Technol.* **1994**, *28*, 320.

(4) Wallington, T. J.; Japar, S. M. *J. Atmos. Chem.* **1989**, *9*, 399.

(5) Hansen, K. B.; Wilbrandt, R.; Pagsberg, P. *Rev. Sci. Instrum.* **1979**, *50*, 1532.

(6) Ellermann, T; Sehested, J; Nielsen, O. J.; Pagsberg, P.; Wallington, T. J. *Chem. Phys. Lett.* **1994**, *218*, 287.

(7) Wallington, T. J.; Dagaut, P.; Kurylo, M. *J. Chem. Rev.* **1992**, *92*, 667.

(8) Wallington, T. J.; Ellermann, T.; Nielsen, O. J. *Res. Chem. Intermed.* **1994**, *20*, 265.

(9) Wallington, T. J.; Hurley, M. D.; Shi, J.; Maricq, M. M.; Sehested, J.; Nielsen, O. J.; Ellermann, T. *Int. J. Chem. Kinet.* **1993**, *25*, 651.

(10) Møgelberg, T. E.; Nielsen, O. J.; Sehested, J.; Wallington, T. J.; Hurley, M. D. *J. Phys. Chem.* **1995**, *99*, 5373.

(11) Nielsen, O. J.; Gamborg, E.; Sehested, J.; Wallington, T. J.; Hurley, M. D. *J. Phys. Chem.* **1994**, *98*, 9518.

(12) Møgelberg, T. E.; Platz, J.; Nielsen, O. J.; Wallington, T. J. *J. Phys. Chem.* **1995**, *99*, 5373.

(13) Sehested, J.; Nielsen, O. J.; Wallington, T. J. *Chem. Phys. Lett.* **1993**, *213*, 457.

(14) Zabel, F.; Kirchner, F.; Becker, K. H. *Int. J. Chem. Kinet.* **1988**, *20*, 827.

(15) Sehested, J. *Int. J. Chem. Kinet.* **1994**, *26*, 1023.

(16) Wallington, T. J.; Ellermann, T.; Nielsen, O. J.; Sehested, J. *J. Phys. Chem.* **1994**, *98*, 2346.

(17) Møgelberg, T. E.; Feilberg, A.; Giessing A. M. B.; Sehested, J.; Bilde, M.; Wallington, T. J.; Nielsen, O. J. *J. Phys. Chem.* **1995**, *99*, 17386.

(18) Wallington, T. J.; Nielsen, O. J. *Chem. Phys. Lett.* **1991**, *187*, 33.

(19) Sehested, J. *Int. J. Chem. Kinet.* **1994**, *26*, 1023.

(20) Kaiser, E. W.; Wallington, T. J.; Hurley, M. D. *Int. J. Chem. Kinet.* **1995**, *27*, 205.

(21) Lightfoot, P. D.; Cox, R. A.; Crowley, J. N.; Destriau. M.; Hayman, G. D.; Jenkin, K. E.; Moorgat, G. K.; Zabel, F. *Atmos. Environ.* **1992**, *26A*, 1805.

(22) Wallington, T. J.; Hurley, M. D. *Chem. Phys. Lett.* **1992**, *189*, 437.

(23) Sehested, J.; Ellermann, T.; Nielsen, O. J.; Wallington, T. J.; Hurley, M. D. *Int. J. Chem. Kinet.* **1993**, *25*, 701.

(24) Edney, E. O.; Driscoll, D. J. *Int. J. Chem. Kinet.* **1992**, *24*, 1067.

(25) Tuazon, E. C.; Atkinson, R. *J. Atmos. Chem.* **1993**, *16*, 301.

(26) Atkinson, R.; Baulch, D. L.; Cox, R. A.; Hampson, R. F.; Kerr, J. A.; Troe, J. *J. Phys. Chem. Ref. Data* **1992**, *21*, 1125.

(27) Percival, C. J.; Marston, G.; Wayne, R. P. *Atmos. Environ.* **1995**, *29*, 305.

(28) Derwent, R. G.; Volz-Thomas, A.; Prather, M. J., World Meteorological Organization Global Ozone Research and Monitoring Project, Report No. 20; *Scientific Assessment of Stratospheric Ozone*, 1989; Vol. II, p 124.

(29) Wallington, T. J.; Schneider, W. F.; Sehested, J.; Nielsen, O. J. *Faraday Discuss.* **1996**, *100*, 55.

(30) Intergovernmental Panel on Climate Change. *Climate Change 1994*; Cambridge University Press: UK, 1995.

JP952769H